Modeling transient particle transport in transient indoor airflow by fast fluid dynamics with the Markov chain method

Wei Liu[a], Twan van Hooff[b,c], Yuting An[d], Simon Hu[e], Chun Chen[d,*]

[a] *Division of Sustainable Buildings, Department of Civil and Architectural Engineering, KTH Royal Institute of Technology, Brinellvägen 23, Stockholm, 100 44, Sweden*
[b] *Department of the Built Environment, Eindhoven University of Technology, P.O. Box 513, 5600, MB Eindhoven, the Netherlands*
[c] *Department of Civil Engineering, KU Leuven, Kasteelpark Arenberg 40 - Bus 2447, 3001 Leuven, Belgium*
[d] *Department of Mechanical and Automation Engineering, The Chinese University of Hong Kong, Shatin, N.T., 999077, Hong Kong SAR, China*
[e] *School of Civil Engineering, ZJU-UIUC Institute, Zhejiang University, Haining, 314400, China*

Abstract

It is crucial to acurately and efficiently predict the transient particle transport in indoor environments in order to improve air distribution design and reduce health risks. For the steady-state indoor airflow, our previous studies have found that the integrated fast fluid dynamics (FFD) + Markov chain model increased the speed of calculation by around 7.0 times compared to the combination of computational fluid dynamics (CFD) + Eulerian model and CFD + Lagrangian model, while a similar accuracy is obtained. However, the indoor airflow could be transient, if there is human behavior like coughing or sneezing, opening the door, and supplying the air periodically. Therefore, this study developed an FFD + Markov chain model solver for predicting transient particle transport in transient indoor airflow in OpenFOAM. This investigation used two cases, transient particle transport in a ventilated two-zone chamber and a chamber with periodic air supply, to validate the model. In the first case, the validation used experimental data from literature and showed that the predicted particle

*Corresponding author
Email address: chunchen@mae.cuhk.edu.hk (Chun Chen)

concentration by FFD + Markov chain model matched well with the experimental data. Besides, it had similar accuracy as the FFD + Eulerian model and the CFD + Eulerian model. In the second case, the prediction by large eddy simulation (LES) was used for validating the FFD. The performance of the Markov chain model was compared with the Eulerian model. Again, this study found the FFD had similar accuracy with CFD in predicting the airflow, and the predicted particle concentration by the Markov chain model agreed well with that by the Eulerian model. For both cases, the FFD + Markov chain model requires a similar computing time with the FFD + Eulerian model if the same time step size was used.

Keywords: fast fluid dynamics, Markov chain model, transient, indoor particle, periodic

---

1. Introduction

In recent decades, major outbreaks of airborne infectious diseases, such as severe acute respiratory syndrome (SARS) [1, 2], influenza A virus subtype H1N1 (H1N1) [3], and coronavirus disease 2019 (COVID-19) [4], have occurred in indoor environments. The index person can exhale droplets containing infectious virus through coughing or sneezing [5, 6]. The droplets quickly evaporate and the droplet nuclei can be transported via the air in indoor environments [7]. These airborne infectious particles may be inhaled by the receptors and cause infection [8]. It has been proven that the air distribution is strongly associated with the airborne infectious particle transport indoors [9]. Therefore, it is crucial to predict the particle transport in indoor environments to support the air distribution design for reducing the infection risks.

Computational fluid dynamics (CFD) has been widely used in predicting indoor particle transport. For example, Chen et al. [10] used the RNG $k-\varepsilon$ model with Lagrangian tracking to calculate the patient-to-dentist particle transport in a dental clinic. Gao et al. [11] applied the similar method to investigate the lock-up phenomenon of human exhaled droplets under a displacement ven-

tilated room. You et al. [12] used a hybrid SST $k-\omega$ and RNG $k-\varepsilon$ turbulence model with the Eulerian approach to calculate the person-to-person contaminant transport in aircraft cabins with different air distribution systems. These studies assumed the airflow field to be steady, while the particle transport is transient. In general, the calculation of the transient particle transport requires more computing time than that of the steady-state airflow field due to the large number of time steps [13].

Note that the exhaled airflow such as a cough or a sneeze is also transient in nature. Therefore, to improve the accuracy of predictions, researchers have also conducted numerical simulations for transient particle transport in transient exhaled airflow. For instance, Gupta et al. [14] investigated the exhaled droplet dispersion in an aircraft cabin by considering a coughed airflow profile. Zhang and Li [15] calculated the dispersion of droplets from a cough in a fully-occupied high-speed rail cabin using the same cough profile. Chen et al. [16] numerically investigated the transport of exhaled particles from a single cough with the mouth covered. For a single cough or sneeze, although the exhaled airflow is transient, the duration of the transient airflow is much shorter than that of the particle dispersion in the air [16]. After the local disturbance of the cough or sneeze disappears, the airflow can be regarded as steady-state for the remaining period [17]. Therefore, the extra computing time for the transient exhaled airflow may not be significant.

In recent years, unsteady airflow distribution systems have been proposed to improve the effectiveness of indoor air pollutant removal. For example, Sattari and Sandberg [18] and Fallenius et al. [19] performed particle image velocimetry (PIV) measurements of a ventilation flow which was driven by a wall jet with a constant supply and one with a periodic velocity at 0.3, 0.4 and 0.5 Hz. Hooff and Blocken [20] numerically studied the impact of the frequency and amplitude of the periodic sine function for air supplies on the ventilation performance. In these cases, both the airflow and particle transport were transient throughout the whole calculation period, which would significantly increase the computing cost. Therefore, it is worthwhile to develop a new model for accelerating the

calculations of transient particle transport in transient airflow in indoor environments.

For airflow calculations, fast fluid dynamics (FFD) has been proven to be faster than CFD with comparable accuracy [21, 22, 23, 24, 25]. For instance, Liu et al. [23] found that FFD was about 20 times faster than CFD with similar accuracy. For transient particle transport, the Markov chain model has also been proven to be faster than the Eulerian and Lagrangian models [26, 27, 28, 29, 30, 31]. For example, Chen et al. [27] reported that the Markov chain model was more than 6 times faster than the Eulerian and Lagrangian models. Therefore, this study aims to develop a FFD + Markov chain model solver for transient particle transport in transient indoor airflow in OpenFOAM, an open-source CFD toolbox. This investigation used two cases, transient particle transport in a ventilated two-zone chamber and a chamber with periodic air supply, to validate the model. The accuracy and sensitivity to the time step size of the FFD + Markov chain model were compared with that of the FFD + Eulerian model to explore the advantages and disadvantages of the proposed FFD + Markov chain model.

2. Methodologies

In order to predict the transient particle transport in transient indoor airflow, in each time step, this study used FFD to predict the airflow and Markov chain model to predict the particle transport in sequence. This section thus briefly introduces FFD and Markov chain model and then focuses on the integration of the two methods.

2.1. Fast fluid dynamics

The FFD in this study uses a two-step, time splitting scheme to solve the momentum equations of the time-dependent Navier-Stokes equations. With the air velocity U_i^n and p^n pressure at the current time step, FFD firstly solves the convection, diffusion, and source terms to obtain an intermediate air velocity

U^* in Eq. (1).

$$\frac{U_i^* - U_i^n}{\Delta t} = -\frac{1}{\rho}\frac{\partial p^n}{\partial x_i} - U_j^n \frac{\partial U_i^*}{\partial x_j} + \nu \frac{\partial^2 U_i^*}{\partial x_j \partial x_j} + \frac{1}{\rho} F_i \tag{1}$$

where t is the time, ρ is the air density, F_i the i_{th} component of the body forces; ν the effective viscosity. By adopting a standard incremental pressure-correction (SIPC) scheme [32, 33], the pressure gradient is included in the source term. The FFD then solves the pressure difference term together with the continuity equation by a pressure projection method [34] in Eq. (2) for calculating the pressure p^{n+1}.

$$\left.\begin{array}{c} \frac{U_i^{n+1} - U_i^*}{\Delta t} = -\frac{1}{\rho}\frac{\partial (p^{n+1} - p^n)}{\partial x_i} \\ \frac{\partial U_i^{n+1}}{\partial x_i} = 0 \end{array}\right\} \Rightarrow \frac{\partial^2 (p^{n+1} - p^n)}{\partial x_i \partial x_i} = \frac{\rho}{\Delta t}\frac{\partial U_i^*}{\partial x_i} \tag{2}$$

The pressure p^{n+1} will be used to calculate the air velocity at the next time step U_i^{n+1} by using the equation for pressure difference term in Eq. (3). The readers can refer to [23] for the detail deductions.

$$\frac{U_i^{n+1} - U_i^*}{\Delta t} = -\frac{1}{\rho}\frac{\partial (p^{n+1} - p^n)}{\partial x_i} \Rightarrow U_i^{n+1} = U_i^* - \frac{\Delta t}{\rho}\frac{\partial (p^{n+1} - p^n)}{\partial x_i} \tag{3}$$

2.2. Markov chain model

The Markov chain model calculates the particle transport by the principle of Lagrangian model on the Eulerian grid. By using a matrix of particle transition probabilities, with $P_{i,i}$ representing the probability of particle's remaining in the current cell i and $P_{nb,i}$ representing the probability of particle's moving from neighboring cells (nb) to cell i, the number of particles in grid cell (N_i) after a time step (Δt) could be calculated by:

$$N_i(t + \Delta t) = N_i(t) P_{i,i} + \sum_{nb} N_{nb} P_{nb,i} \tag{4}$$

According to [27], the transition probability $P_{i,i}$ is determined by solving the particle mass balance equation:

$$P_{i,i} = \exp(-\sum \frac{Q_{i,nb}}{V_i} \Delta t) \tag{5}$$

where $Q_{i,nb}$ is the mass flux from a neighboring cell to cell i and V_i is the volume of cell i. Then the transition probability $P_{i,nb}$ could be determined by:

$$P_{i,nb} = \frac{Q_{i,nb}}{\sum_{nb} Q_{i,nb}}(1 - P_{i,i}) \tag{6}$$

Once all the $P_{i,nb}$ are determined, the $P_{nb,i}$ are known accordingly. Basically, the Markov chain model calculates the number of particles in each grid cell, then the particle concentration could be determined by dividing the particle number (N_i) by cell volume (V_i). The readers can refer to [27] for the detail deductions.

2.3. Integration of FFD with Markov chain model

Due to the transient airflow, the mass flux on the grid cell faces are transient, which further leads to transient particle transition probabilities. Therefore, in each time step, the FFD + Markov chain model first solves Eqs. (1), (2), and (3) in sequence to obtain the air velocity U^n as shown in Figure 1. To simulate the turbulence, this study solves the renormalization group (RNG) $k - \varepsilon$ model equations. The RNG $k - \varepsilon$ model is one of the best Reynolds-averaged Navier–Stokes (RANS) turbulence models for predicting the indoor airflow [35, 36].

With the predicted airflow, the combined method then constructs the matrix of particle transition probabilities by using the Eqs. (5) and (6). Finally, the particle number distribution could be calculated by Eq. (4) and the particle concentration could be further obtained by dividing N_i by cell volume V_i. The FFD + Markov chain model for predicting transient particle transport in transient indoor airflow was implemented in OpenFOAM [37].

Please note that the matrix of particle transition probabilities need to be calculated in each time step due to transient indoor airflow. For steady-state airflow, the matrix of particle transition probabilities will be constructed only once after the airflow is predicted. Then Eq. (4) is solved to predict the transient particle transport. Therefore, predicting the transient particle transport in steady-state airflow by the Markov chain model could be very efficient [25, 28]. However, for predicting the transient particle transport in transient airflow, the

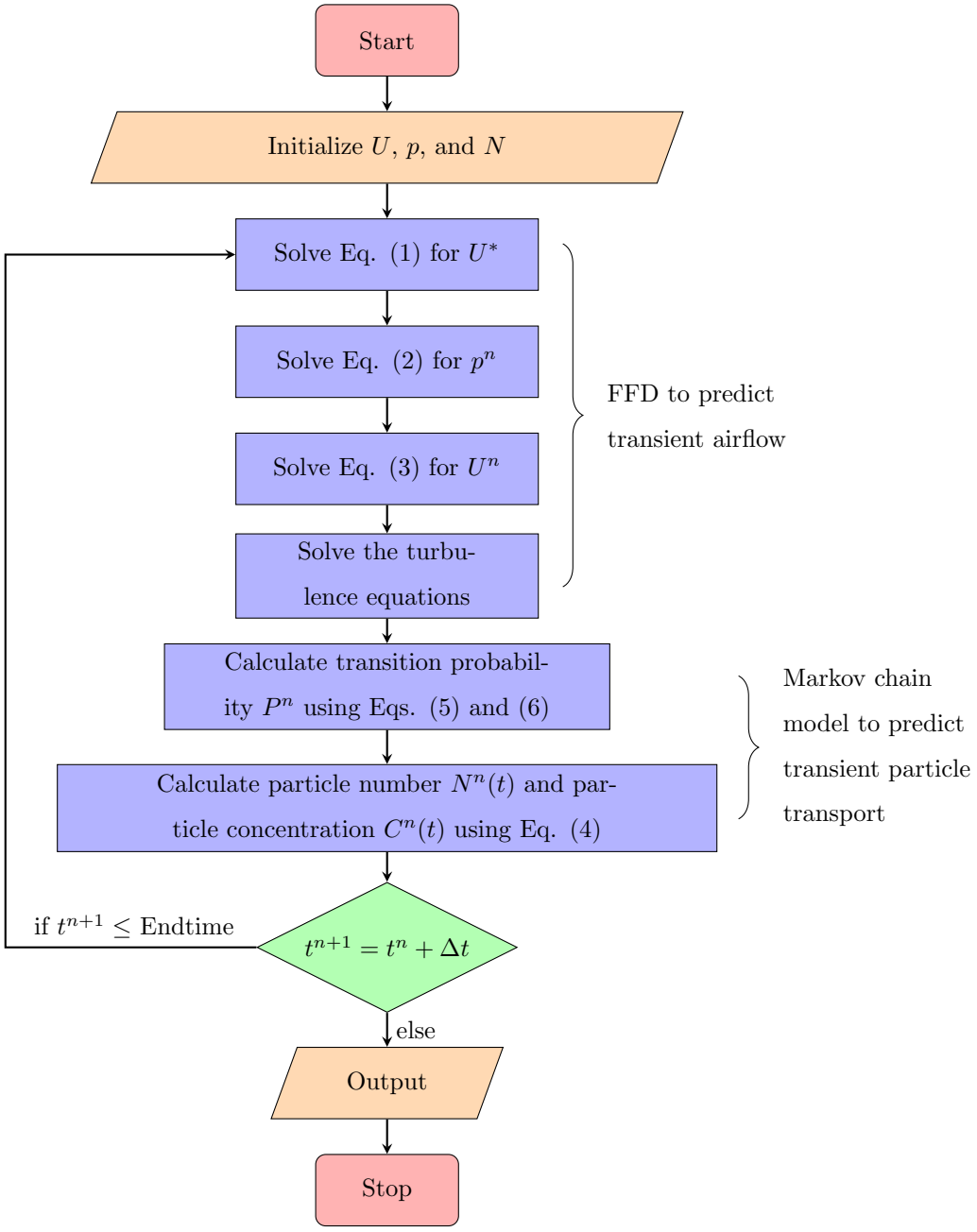

Figure 1: Solution flow chart of the FFD + Markov chain model

efficiency of the Markov chain model would decrease due to solving Eqs. (5) and (6) in each time step.

3. Results

Due to the ndifficulty and complexity in measuring transient particle transport with transient indoor airflow, this study used two cases from literature to test the accuracy and efficiency of the FFD + Markov chain model. The first case was transient particle transport experiment in a ventilated two-zone chamber [38]. The second case was transient particle transport in a ventilated room with periodic air supplies [20]. This case had predicted airflow by sophisticated numerical tools for validating the FFD in predicting the transient airflow. This study then compared the Markov chain model with the traditional Eulerian model in predicting the transient particle transport.

3.1. Case 1: particle transport in a two-zone ventilated chamber

Figure 2(a) shows the geometry of a two-zone ventilated chamber with the dimension $5 \times 2.4 \times 3\ m^3$. The two zones were separated by a partition with a sliding door ($0.95 \times 0.7\ (y \times z)\ m^2$). There was an inlet ($0.5 \times 1.0\ (y \times z)\ m^2$) located on the left wall of zone 1 and an outlet ($0.5 \times 1.0\ (y \times z)\ m^2$) located on the right wall of zone 2. Initially, the door was closed and air supply was off. The zone 1 was injected by smoke particles in a range of 0.5-5 μm. At $t = 0$, the door was opened and air was supplied from the inlet at $U_x = 0.09216$ $m/s, U_y = 0$, and $U_z = 0$. The corresponding air change rate per hour (ACH) was 9.216 h^{-1} or time constant was $\tau = 390\ s$. The experiment measured the particle concentration at the center of each zone (green dots in Figure 2(a)) for 26 minutes [38].

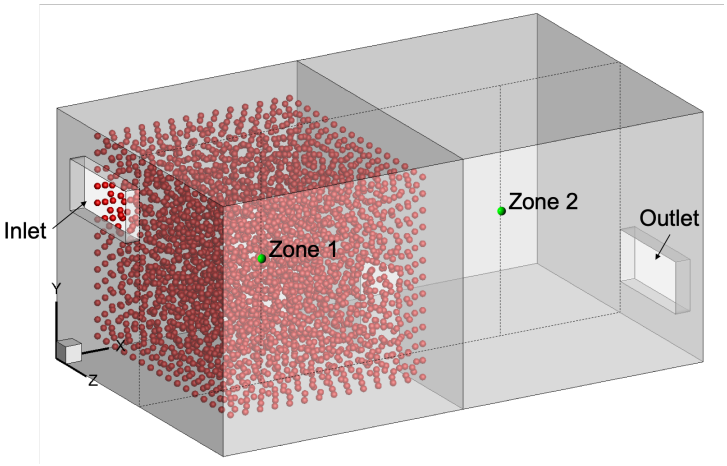

(a) Geometry

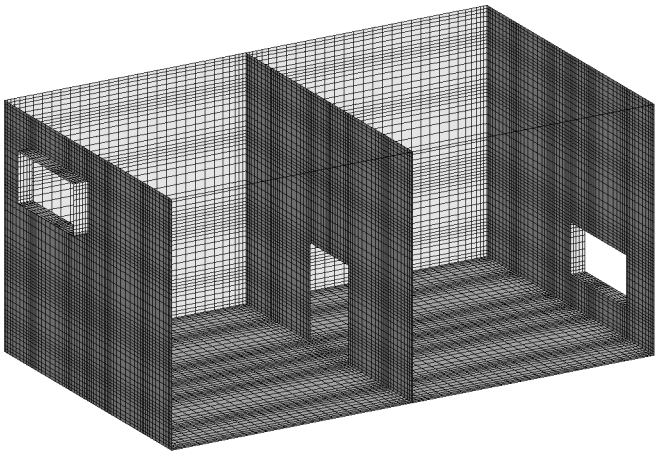

(b) Mesh

Figure 2: Layout of a two-zone ventilated chamber [38]

The FFD simulation of the transient airflow exactly used the boundary conditions from the experiment, except assuming the turbulence intensity of the inlet air to be 10% for calculating the inlet turbulence kinetic energy k and turbulence dissipation rate ε, which were not provided in the experiment. Besides, this Markov chain model does not consider the inertial effects of the particles [27, 39]. This investigation first conducted grid independence test with four

grid resolutions: 29844 (mesh 1), 74136 (mesh 2), 220550 (mesh 3), and 472050 (mesh 4). This study ran the FFD + Markov chain model for 2τ with a time step size $\Delta t = 0.01\ s$. The time step size was the same with the value used in [38]. Figure 3 compares the predicted air velocity profiles at two positions after 2τ. Positions 1 and 2 are the vertical lines at the center of zone 1 and zone 2, respectively. Since the predictions with mesh 3 agreed well with that with mesh 4, the following simulations used mesh 3 as shown in Figure 2(b).

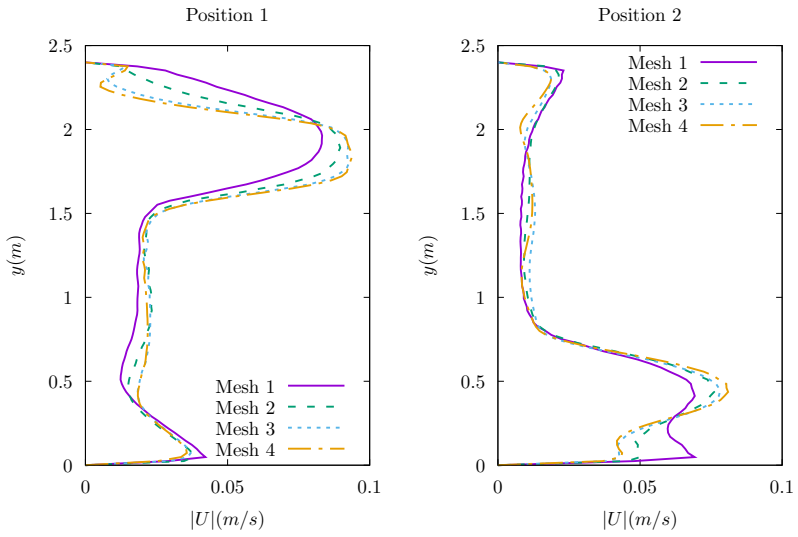

Figure 3: Grid independence test for case 1

With mesh 3, this study ran the FFD + Markov chain model for 27 minutes with a time step size $\Delta t = 0.01\ s$. The prediction by CFD + Eulerian model with was also conducted for comparison. Due to the particle size was small, the Eulerian model used a drift-flux model [40], which is a simplified Eulerian two-phase flow model. The CFD simulation used the SIMPLE algorithm to couple the air pressure and velocity. The other setups such as numerical schemes, time step size, boundary conditions, and turbulence model, etc. of the CFD simulation were the same with that of the FFD simulation. Figure 4 compares the predicted particle concentration with the experiment data in zone 1 and zone

2. In zone 1, all the predictions were similar and agreed well with the experimental data in the first 4 minutes. Afterwards, all the predictions were different and the predictions by FFD + Eulerian model had the best agreement with the measured value. A possible reason was the difference in predicting the airflow by CFD and FFD, as well as the difference in predicting the particle transport by Eulerian model and Markov chain model. In zone 2, all the simulations over predicted the drop of particle concentration around $t = 2.5\ min$. This is because the strong unsteady feature of the airflow in the beginning, which further affect the accuracy in predicting the particle transport. Afterwards, predicted particle concentration by CFD + Eulerian model and FFD + Markov chain model were similar and agreed well with the experimental data. The FFD + Eulerian model lower predicted the of particle concentration overall.

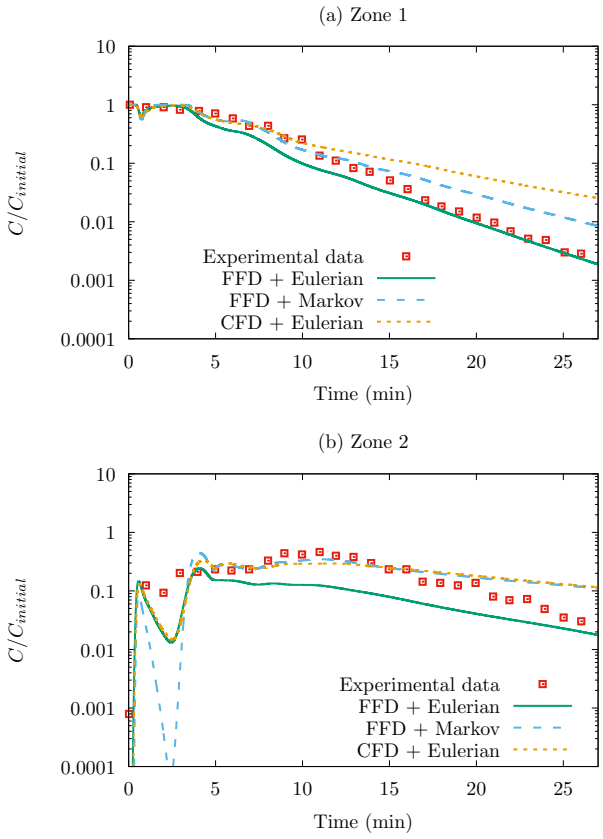

Figure 4: Particle concentrations vs. time in zone 1 and zone 2 for case 1

This study further investigated the impact of time step size on the accuracy of the predictions. With the extra four time steps: $\Delta t = 0.1, 1.0, 2.0$, and 5.0 s, FFD was used for predicting the airflow and Markov chain model and Eulerian model were used for predicting the particle transport, respectively. The corresponding mean and maximum Courant numbers (Co) were provided in Table 1. This study did not test time step size greater than 5.0 s since the Co_{mean} for $\Delta t = 5.0$ s was much greater than one. Figure 5 shows the predicted particle concentration vs. time for FFD + Markov chain model. One can notice the almost identical predictions with $\Delta t = 0.01, 0.1$, and 1.0 s, which could be regarded as time-step-size independent. Then the prediction with $\Delta t = 2.$ s

showed minor difference with those predicted with smaller time step sizes. With $\Delta t = 5.0\ s$, the FFD + Markov chain model was unable to predict the correct particle concentrations. Figure 6 shows the predicted particle concentration vs. time for FFD + Eulerian model. It was found that the predictions with $\Delta t = 0.01$, $0.1\ s$, $1.0\ s$, and $2.0\ s$ were identical. Again, with $\Delta t = 5.0\ s$, the FFD + Eulerian model was unable to predict the correct particle concentrations.

$\Delta t(s)$	0.01	0.1	1.0	2.0	5.0
Co_{mean}	0.00593	0.0594	0.594	1.185	2.952
Co_{max}	0.0609	0.609	6.166	12.471	32.155

Table 1: Tested time step sizes and the corresponding Courant numbers (Co) for case 1

(a) Zone 1

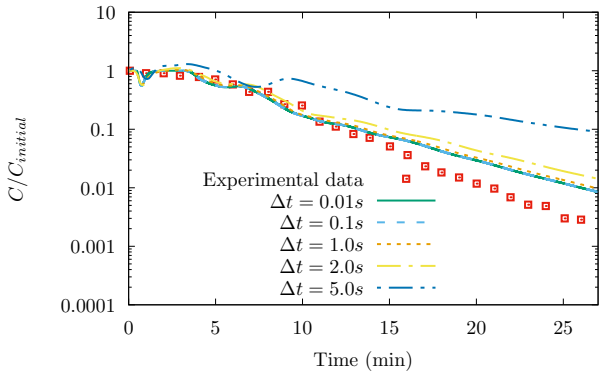

(b) Zone 2

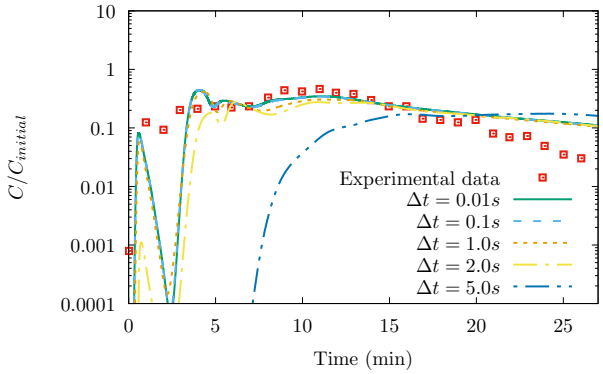

Figure 5: Effect of the time step size for FFD + Markov in case 1

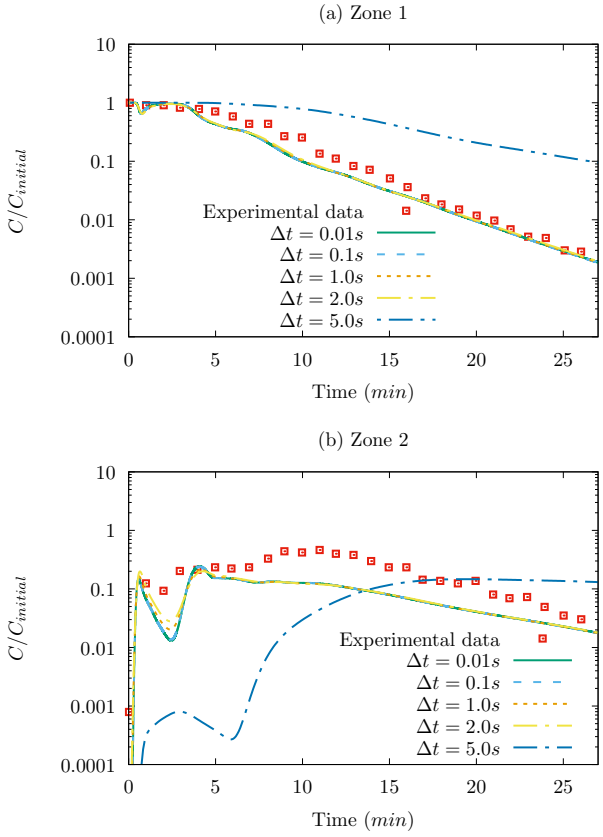

Figure 6: Effect of the time step size for FFD + Eulerian in case 1

To further identify the reason for the wrong predictions with $\Delta t = 5.0\ s$, Figure 7 compares the predicted airflow by FFD with different time step sizes in the mid-section of the room. Since this case was iso-thermal, the inlet jet flowed horizontally to the partition wall and then flowed downward to the door. After the door, the air flowed along the floor to the exhaust. It is clear that the flow fields changed a lot in the beginning and the greater the time step size, the more diffusive the predicted airflow in the first 50 s. With $\Delta t = 5.0\ s$, the predicted airflow in the first 50 s was not sufficient accurate for predicting the particle transport. However, at $t = 100\ s$ and $t = 200\ s$, the predicted airflow with $\Delta t = 5.0\ s$ agreed well with those predicted with smaller time step sizes.

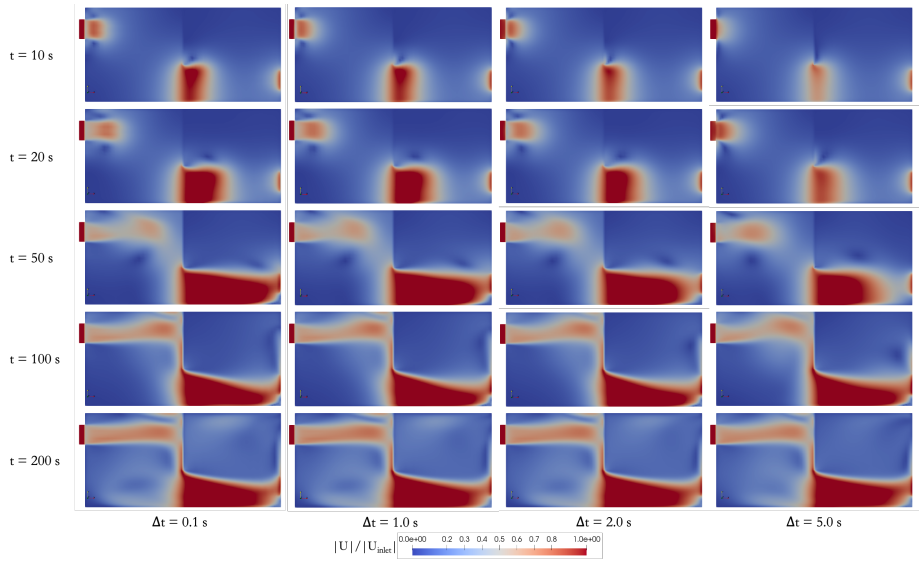

Figure 7: Predicted airflow by FFD with different time step sizes in the mid-section of the room in case 1

With $\Delta t = 0.1\ s$, Figure 8 shows the predicted transient particle concentration distributions by the Markov chain model and Eulerian model in the mid-section of the room. The particles in zone 1 moved along the airflow to zone 2. Both the Markov chain model and Eulerian model was able to predict the residual particles above inlet in zone 1 and the recirculated particles in zone 2. In general, the predicted particle concentration by the Markov chain model agreed well with that by the Eulerian model.

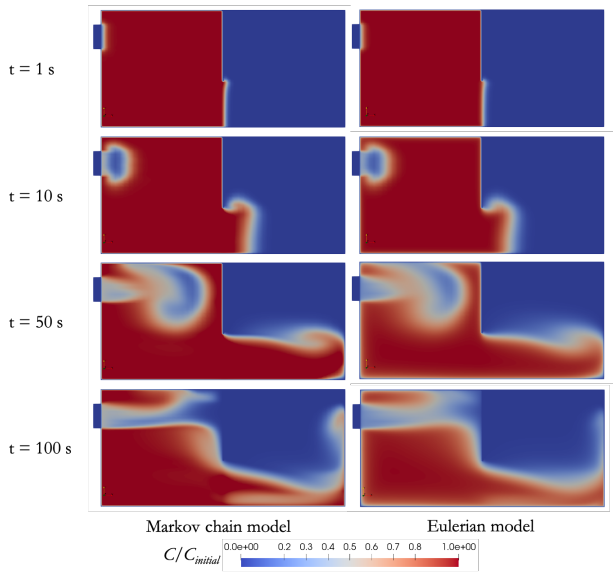

Figure 8: Predicted transient particle concentration distributions by the Markov chain model and Eulerian model in the mid-section of the room in case 1

3.2. Case 2: particle transport in a ventilated room with periodic air supplies

The second case was particle transport in a ventilated room ($9 \times 3 \times 3\ m^3$ ($x \times y \times z$)) with two inlets and two outlets [20]. As shown in Figure 9(a), the air was supplied by two inlets ($0.168 \times 3\ m^2$ ($y \times z$)) oppositely located in the upper part of the side walls. Accordingly, the air was exhausted by two outlets ($0.48 \times 3\ m^2$ ($y \times z$)) oppositely located in the floor level of the side walls. The air supply velocities for the left and right inlets were:

$$U_{inlet,x}^{left}(t) = U_0(1 + \sin(2\pi t/T)) \tag{7}$$

$$U_{inlet,x}^{right}(t) = U_0(1 - \sin(2\pi t/T)) \tag{8}$$

where the period was $T = 0.4\tau$ with the room time constant $\tau = 160.71\ s$ and $U_0 = 0.5\ m/s$. According to [20], the turbulence intensity (TI) and turbulent viscosity ratio $\frac{\mu_t}{\mu}$ of the inlet jets were assumed to be 10% and 10, respectively.

Then the inlet k and ε could be calculated by:

$$k = \frac{3}{2}(U_{inlet,x}(t)TI)^2 \tag{9}$$

$$\varepsilon = \rho C_\mu \frac{k^2}{\mu}\left(\frac{\mu_t}{\mu}\right)^{-1} \tag{10}$$

where C_μ is an empirical constant specified in the turbulence model. For the RNG $k-\varepsilon$ model used in this study, the value C_μ of was 0.0845.

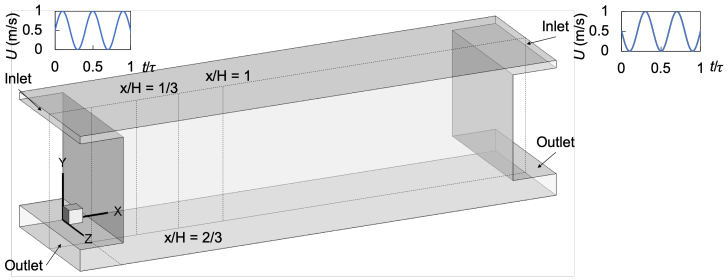

(a) Geometry

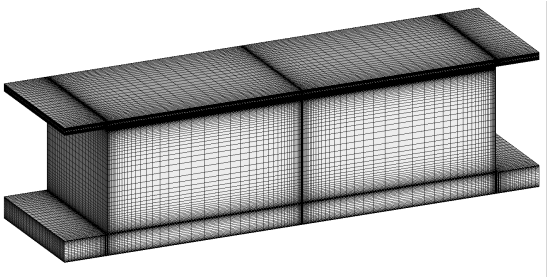

(b) Mesh

Figure 9: Layout of a ventilated room with periodic air supplies [20]

Due to complex air supply conditions in this case, this study first validated FFD in predicting the airflow. The validation used the numerical results by unsteady Reynolds-averaged Navier-Stokes (URANS) CFD simulations using the RNG $k-\varepsilon$ turbulence model and a large-eddy simulation (LES) using the dynamic Smagorinksy subgrid-scale model from [20]. Accordingly, the FFD simulation used the same mesh (505,760 hexahedral cells) as shown in Figure

9(b) and time step size ($\Delta t = 0.1\ s$) with those used by the URANS simulations. The time step size of LES was $\Delta t = 0.01\ s$.

Figure 10 compares the dimensionless mean velocity magnitude ($|U|/U_0$) along three vertical lines, $x/H = 1/3$, $x/H = 2/3$, and $x/H = 1$, in the vertical center plane, where $H = 3\ m$ is the room height. The mean air velocity used the predicted results between 2τ and 33τ. One can notice minor differences between predicted air velocity profiles by FFD, URANS, and LES simulations. Therefore, the FFD simulations could be accurate in predicting the complex transient airflow.

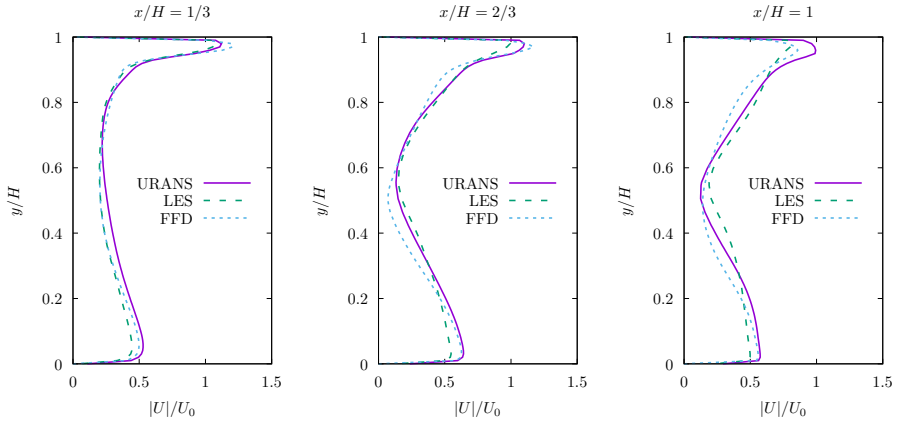

Figure 10: Dimensionless mean velocity magnitude ($|U|/0.5$) (mean data between 2τ and 33τ or 320 s and 5320 s) along three vertical lines in the vertical center plane in case 2.

In order to compare the performance of Markov chain model and Eulerian model, this study injected particles at the center of the room with the height $y = 1.7\ m$ to simulate the exhaled particles from an occupant. The particles were released between $t = 2\tau$ and $t = 2\tau + 1\ s$. The size of the particles was assumed to be 3 μm and the inertial force was neglected. Figure 11 shows the predicted airflow by FFD and transient particle concentration distributions by the Markov chain model and Eulerian model in the mid-section of the room. The particle concentration was normalized by the maximal concentration at

the source. The air velocity of the jet from the left inlet increased while that of the jet from the right inlet decreased. Then the big air circulation in the right side vanished gradually and a big air circulation came out in the left side. Although the airflow fields changed significantly over time, the Markov chain model and Eulerian model both predicted that the particles moved downward to the floor and then traveled along the floor to the right outlet. The Markov chain model agreed well with the Eulerian model in capturing the general trend of the transient particle transport in the room.

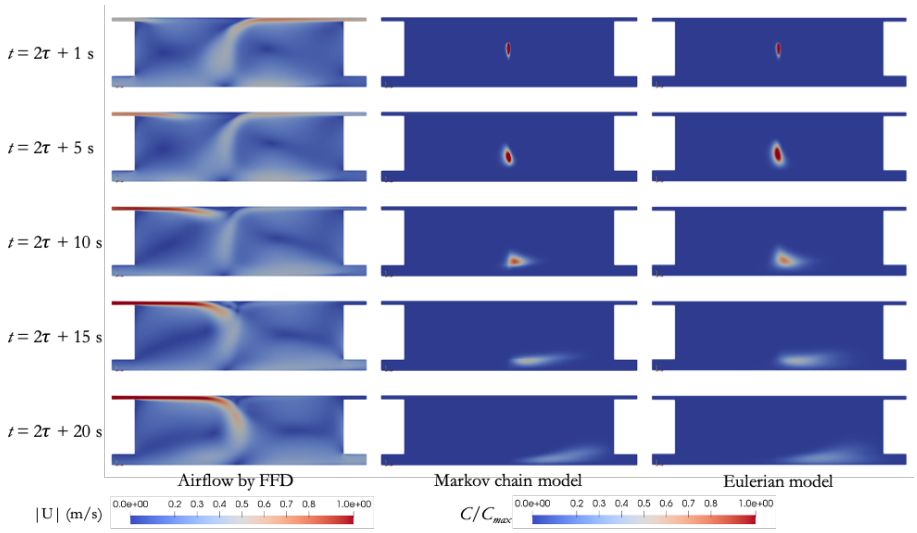

Figure 11: Predicted airflow by FFD and transient particle concentration distributions by the Markov chain model and Eulerian model in the mid-section of the room

This study conducted further simulations with greater time step sizes: $\Delta t = 0.2\ s$ and $\Delta t = 0.5\ s$. Table 2 summarizes the tested time step sizes and the corresponding Courant numbers (Co). With $\Delta t = 0.5\ s$, the mean Courant number was close to two and the maximal Courant number was extremely large. This was due to the fine mesh close to the air supply inlets, walls, and then central domain where the two inlet jets meet. Figure 12 shows the predicted airflow by FFD with different time step sizes in the mid-section of the room.

At each time moment, the greater the time step size, the less developed the inlet jet. Although the Co_{mean} of the prediction with $\Delta t = 0.2\ s$ was less than 1, the predicted airflow had noticeable difference from the one predicted with $\Delta t = 0.1\ s$. Therefore, this study did not consider the prediction of particle transport with time step size greater than $\Delta t = 0.1\ s$.

$\Delta t(s)$	0.1	0.2	0.5
Co_{mean}	0.377	0.765	1.825
Co_{max}	29.133	67.055	151.036

Table 2: Tested time step sizes and the corresponding Courant numbers (Co) for case 2

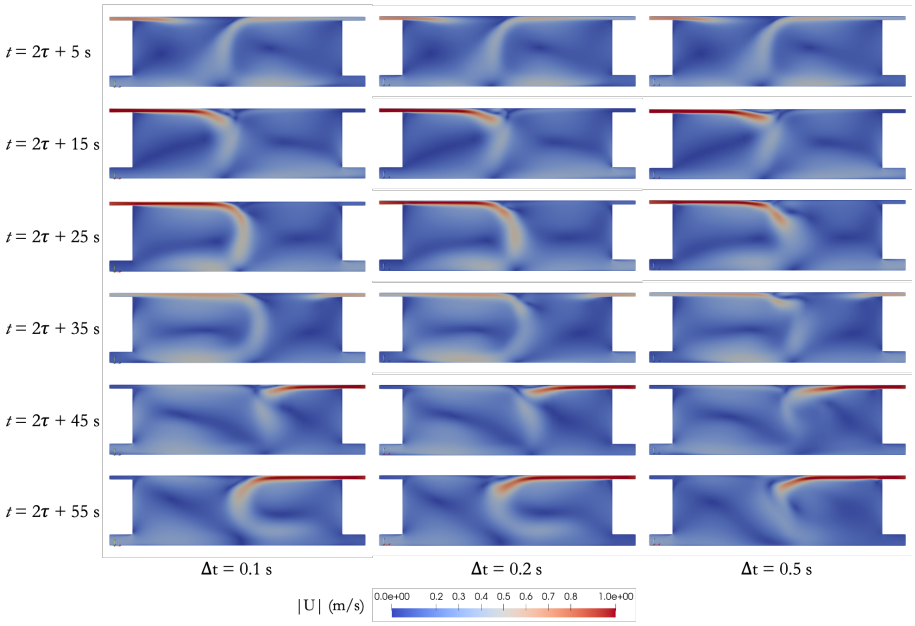

Figure 12: Predicted airflow by FFD with different time step sizes in the mid-section of the room in case 2

4. Discussions

This investigation ran the numerical simulations in case 1 and the FFD simulations in case 2 with an Intel Xeon platinum 8179M processor with the frequency of 3.0 GHz. All the FFD simulations were ran with one core. Since the CFD simulation was time consuming, this study ran the CFD simulations for case 1 with eight cores and the computing time was 69.5 hours. To compare the computing time, our test found that using eight cores would speed up the computation with one core by 6.2 times for case 1. Therefore, the computing time of CFD simulation for case 1 with one core was estimated to be 429.4 hours. Figure 13 shows the computing time for predicting the airflow and particle transport. In predicting the airflow, the FFD was 8.8 times faster than the CFD. In predicting the particle transport, the Markov chain model consumes twice the computing time of the Eulerian model. Since the computing time of predicting the particle transport was one order of magnitude less than that of predicting the airflow, further acceleration of the computing speed should focus on predicting the airflow.

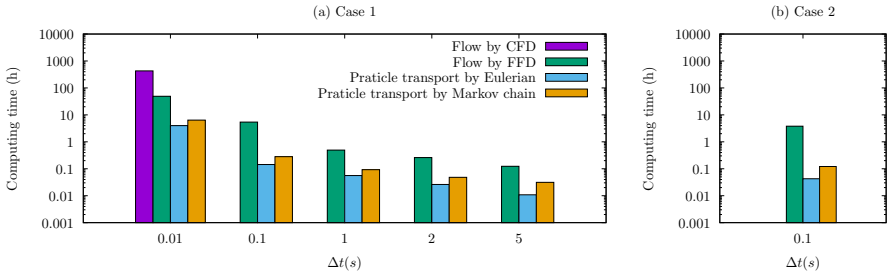

Figure 13: Computing time for predicting the airflow and particle transport

According to [29], the ideal time step size for constructing the matrix of particle transition probabilities is:

$$\Delta t_{ideal} = \frac{3}{4}\frac{h}{|U|} \tag{11}$$

However, our tests indicated that the performance of the Markov chain model was dependent on the accuracy in predicting the transient airflow. As long as the FFD simulations were able to give the accurate airflow, the Markov chain model was capable of predicting the correct particle transport.

The results in this study indicated that the Markov chain model was not faster than the Eulerian model in predicting the transient particle transport in transient airflow. This was because the transition probabilities in the Markov chain model need to be calculated in every time step, the computing cost of which overwhelmed the model's advantage of not requiring iteration. Therefore, to accelerate the Markov chain model, one option is to pre-calculate the transition probabilities under different airflow distributions to form a database. With the pre-calculated database, the Markov chain model can be speeded up without the need of online transition probability calculations. This potential approach deserves further investigation in the future.

5. Conclusions

This investigation combined the FFD and Markov chain model and implemented it in OpenFOAM for predicting the transient particle transport in transient indoor airflow. The developed solver was validated by the airflow and particle transport in a ventilated two-zone room and a ventilated room with periodic air supplies. Not only the performance in predicting the transient particle transport, but also the performance in predicting the transient airflow was tested. The results lead to the following conclusions:

- The FFD + Markov chain model had the similar accuracy with the FFD + Eulerian model in predicting the particle transport;
- The Markov chain model consumes twice the computing time of the Eulerian model. Since the computing time of predicting the particle transport was one order of magnitude less than that of predicting the airflow, the efficiency of the FFD + Markov chain model was almost the same with that of the FFD + Eulerian model;

- The FFD had similar accuracy with CFD in predicting the complex transient indoor airflow and it could be 8.8 times faster in the tested case.

Acknowledgment

This work was supported in part by the National Natural Science Foundation of China (Grant No. 51808487) and the Energimyndigheten (Swedish Energy Agency, grant No. 50057-1). This work was supported in part by the Zhejiang University/University of Illinois at Urbana-Champaign Institute, and was led by Principal Supervisor Simon Hu.

References

[1] S. J. Olsen, H.-L. Chang, T. Y.-Y. Cheung, A. F.-Y. Tang, T. L. Fisk, S. P.-L. Ooi, H.-W. Kuo, D. D.-S. Jiang, K.-T. Chen, J. Lando, et al., Transmission of the severe acute respiratory syndrome on aircraft, New England Journal of Medicine 349 (25) (2003) 2416–2422.

[2] Y. Li, X. Huang, I. Yu, T. Wong, H. Qian, Role of air distribution in sars transmission during the largest nosocomial outbreak in hong kong., Indoor air 15 (2) (2005) 83–95.

[3] S. Cauchemez, C. A. Donnelly, C. Reed, A. C. Ghani, C. Fraser, C. K. Kent, L. Finelli, N. M. Ferguson, Household transmission of 2009 pandemic influenza a (h1n1) virus in the united states, New England Journal of Medicine 361 (27) (2009) 2619–2627.

[4] Y. Liu, Z. Ning, Y. Chen, M. Guo, Y. Liu, N. K. Gali, L. Sun, Y. Duan, J. Cai, D. Westerdahl, X. Liu, K. Xu, K.-f. Ho, H. Kan, Q. Fu, K. Lan, Aerodynamic analysis of sars-cov-2 in two wuhan hospitals, Nature`doi: 10.1038/s41586-020-2271-3`.
URL `https://doi.org/10.1038/s41586-020-2271-3`

[5] C. Y. H. Chao, M. P. Wan, L. Morawska, G. R. Johnson, Z. Ristovski, M. Hargreaves, K. Mengersen, S. Corbett, Y. Li, X. Xie, et al., Characterization of expiration air jets and droplet size distributions immediately at the mouth opening, Journal of Aerosol Science 40 (2) (2009) 122–133.

[6] L. Morawska, G. Johnson, Z. Ristovski, M. Hargreaves, K. Mengersen, S. Corbett, C. Y. H. Chao, Y. Li, D. Katoshevski, Size distribution and sites of origin of droplets expelled from the human respiratory tract during expiratory activities, Journal of Aerosol Science 40 (3) (2009) 256–269.

[7] C. Chen, B. Zhao, Some questions on dispersion of human exhaled droplets in ventilation room: answers from numerical investigation, Indoor Air 20 (2) (2010) 95–111.

[8] M. Nicas, W. W. Nazaroff, A. Hubbard, Toward understanding the risk of secondary airborne infection: emission of respirable pathogens, Journal of occupational and environmental hygiene 2 (3) (2005) 143–154.

[9] Y. Li, G. M. Leung, J. Tang, X. Yang, C. Chao, J. Z. Lin, J. Lu, P. V. Nielsen, J. Niu, H. Qian, et al., Role of ventilation in airborne transmission of infectious agents in the built environment-a multidisciplinary systematic review., Indoor air 17 (1) (2007) 2–18.

[10] C. Chen, B. Zhao, W. Cui, L. Dong, N. An, X. Ouyang, The effectiveness of an air cleaner in controlling droplet/aerosol particle dispersion emitted from a patient's mouth in the indoor environment of dental clinics, Journal of the Royal Society Interface 7 (48) (2010) 1105–1118.

[11] N. Gao, Q. He, J. Niu, Numerical study of the lock-up phenomenon of human exhaled droplets under a displacement ventilated room, in: Building Simulation, Vol. 5, Springer, 2012, pp. 51–60.

[12] R. You, C.-H. Lin, D. Wei, Q. Chen, Evaluating the commercial airliner cabin environment with different air distribution systems, Indoor air 29 (5) (2019) 840–853.

[13] C. Chen, W. Liu, C.-H. Lin, Q. Chen, Accelerating the lagrangian method for modeling transient particle transport in indoor environments, Aerosol Science and Technology 49 (5) (2015) 351–361.

[14] J. K. Gupta, C.-H. Lin, Q. Chen, Transport of expiratory droplets in an aircraft cabin, Indoor Air 21 (1) (2011) 3–11.

[15] L. Zhang, Y. Li, Dispersion of coughed droplets in a fully-occupied high-speed rail cabin, Building and Environment 47 (2012) 58–66.

[16] C. Chen, C.-H. Lin, Z. Jiang, Q. Chen, Simplified models for exhaled airflow from a cough with the mouth covered, Indoor air 24 (6) (2014) 580–591.

[17] C. Chen, W. Liu, F. Li, C.-H. Lin, J. Liu, J. Pei, Q. Chen, A hybrid model for investigating transient particle transport in enclosed environments, Building and Environment 62 (2013) 45–54.

[18] A. Sattari, M. Sandberg, Piv study of ventilation quality in certain occupied regions of a two-dimensional room model with rapidly varying flow rates, International Journal of Ventilation 12 (2) (2013) 187–194.

[19] B. E. Fallenius, A. Sattari, J. H. Fransson, M. Sandberg, Experimental study on the effect of pulsating inflow to an enclosure for improved mixing, International journal of heat and fluid flow 44 (2013) 108–119.

[20] T. van Hooff, B. Blocken, Mixing ventilation driven by two oppositely located supply jets with a time-periodic supply velocity: A numerical analysis using computational fluid dynamics, Indoor and Built Environment (2019) 1420326X19884667.

[21] W. Zuo, Q. Chen, Real-time or faster-than-real-time simulation of airflow in buildings, Indoor air 19 (1) (2009) 33.

[22] W. Liu, M. Jin, C. Chen, R. You, Q. Chen, Implementation of a fast fluid dynamics model in openfoam for simulating indoor airflow, Numerical Heat Transfer, Part A: Applications 69 (7) (2016) 748–762.

[23] W. Liu, R. You, J. Zhang, Q. Chen, Development of a fast fluid dynamics-based adjoint method for the inverse design of indoor environments, Journal of Building Performance Simulation 10 (3) (2017) 326–343.

[24] W. Liu, Q. Chen, Development of adaptive coarse grid generation methods for fast fluid dynamics in simulating indoor airflow, Journal of Building Performance Simulation 11 (4) (2018) 470–484.

[25] W. Liu, R. You, C. Chen, Modeling transient particle transport by fast fluid dynamics with the markov chain method, in: Building Simulation, Vol. 12, Springer, 2019, pp. 881–889.

[26] C. Chen, C.-H. Lin, Z. Long, Q. Chen, Predicting transient particle transport in enclosed environments with the combined computational fluid dynamics and m arkov chain method, Indoor Air 24 (1) (2014) 81–92.

[27] C. Chen, W. Liu, C.-H. Lin, Q. Chen, A markov chain model for predicting transient particle transport in enclosed environments, Building and Environment 90 (2015) 30–36.

[28] C. Chen, W. Liu, C.-H. Lin, Q. Chen, Comparing the markov chain model with the eulerian and lagrangian models for indoor transient particle transport simulations, Aerosol Science and Technology 49 (10) (2015) 857–871.

[29] A. D. Fontanini, U. Vaidya, B. Ganapathysubramanian, Constructing markov matrices for real-time transient contaminant transport analysis for indoor environments, Building and Environment 94 (2015) 68–81.

[30] A. D. Fontanini, U. Vaidya, A. Passalacqua, B. Ganapathysubramanian, Contaminant transport at large courant numbers using markov matrices, Building and Environment 112 (2017) 1–16.

[31] X. Mei, G. Gong, Predicting airborne particle deposition by a modified markov chain model for fast estimation of potential contaminant spread, Atmospheric Environment 185 (2018) 137–146.

[32] K. Goda, A multistep technique with implicit difference schemes for calculating two-or three-dimensional cavity flows, Journal of computational physics 30 (1) (1979) 76–95.

[33] J.-L. Guermond, P. Minev, J. Shen, An overview of projection methods for incompressible flows, Computer methods in applied mechanics and engineering 195 (44-47) (2006) 6011–6045.

[34] A. J. Chorin, A numerical method for solving incompressible viscous flow problems, Journal of computational physics 2 (1) (1967) 12–26.

[35] Z. Zhang, W. Zhang, Z. J. Zhai, Q. Y. Chen, Evaluation of various turbulence models in predicting airflow and turbulence in enclosed environments by cfd: Part 2—comparison with experimental data from literature, Hvac&R Research 13 (6) (2007) 871–886.

[36] B. Blocken, Les over rans in building simulation for outdoor and indoor applications: a foregone conclusion?, in: Building Simulation, Vol. 11, Springer, 2018, pp. 821–870.

[37] H. Jasak, A. Jemcov, Z. Tukovic, et al., Openfoam: A c++ library for complex physics simulations, in: International workshop on coupled methods in numerical dynamics, Vol. 1000, IUC Dubrovnik Croatia, 2007, pp. 1–20.

[38] W. Lu, A. T. Howarth, N. Adam, S. B. Riffat, Modelling and measurement of airflow and aerosol particle distribution in a ventilated two-zone chamber, Building and environment 31 (5) (1996) 417–423.

[39] B. Zhao, C. Chen, Z. Tan, Modeling of ultrafine particle dispersion in indoor environments with an improved drift flux model, Journal of Aerosol Science 40 (1) (2009) 29–43.

[40] F. Chen, C. Simon, A. C. Lai, Modeling particle distribution and deposition in indoor environments with a new drift–flux model, Atmospheric Environment 40 (2) (2006) 357–367.